

## Coarse grained models in Coulomb frustrated phase separation

This article has been downloaded from IOPscience. Please scroll down to see the full text article.

2008 J. Phys.: Condens. Matter 20 434229

(<http://iopscience.iop.org/0953-8984/20/43/434229>)

View [the table of contents for this issue](#), or go to the [journal homepage](#) for more

Download details:

IP Address: 129.252.86.83

The article was downloaded on 29/05/2010 at 16:06

Please note that [terms and conditions apply](#).

## REVIEW ARTICLE

# Coarse grained models in Coulomb frustrated phase separation

C Ortix<sup>1</sup>, J Lorenzana<sup>2,3</sup> and C Di Castro<sup>3</sup>

<sup>1</sup> Dipartimento di Fisica, Università del Salento and INFN Sezione di Lecce,  
Via per Arnesano, 73100 Lecce, Italy

<sup>2</sup> ISC-CNR, Via dei Taurini 19, 00185 Roma, Italy

<sup>3</sup> SMC, INFN-CNR, Dipartimento di Fisica, Università di Roma 'La Sapienza',  
Piazzale Aldo Moro 2, 00185 Roma, Italy

E-mail: [carmine.ortix@le.infn.it](mailto:carmine.ortix@le.infn.it)

Received 7 July 2008

Published 9 October 2008

Online at [stacks.iop.org/JPhysCM/20/434229](http://stacks.iop.org/JPhysCM/20/434229)

## Abstract

Competition between interactions on different length scales leads to self-organized textures in classical as well as quantum systems. This pattern formation phenomenon has been invoked to explain some intriguing properties of a large variety of strongly correlated electronic systems that includes for example high temperature superconductors and colossal magnetoresistance manganites. We classify the more common situations in which Coulomb frustrated phase separation can occur and review their properties.

(Some figures in this article are in colour only in the electronic version)

## 1. Introduction

A large variety of systems with competing short and long range interactions self-organizes in domain patterns [1]. Examples range from ferromagnetic systems [2, 3] to diblock copolymers [4] and, at least theoretically, neutron star matter [5]. Inhomogeneous states display a simple set of predominant morphologies like circular droplets and stripes in two-dimensional (2D) systems, and layers, cylindrical rods and spherical droplets in three-dimensional (3D) systems. This tendency for a common behavior across different systems calls for simple models which neglect the specific details of each system and capture the general properties.

In this work we will discuss phase separation frustrated by the 3D Coulomb interaction in electronic systems, but similar ideas apply also to neutron star matter and diblock copolymers. The tendency for phase separation in electronic systems manifests itself by anomalies in the electronic contribution to the free energy density  $f_e$ . Two kinds of anomalies appear often in strongly correlated systems. The first situation is determined by a negative compressibility region. A notorious example is the uniform electron gas (EG) at low density [6], but this feature appears in several other models [7–15] including neutron star matter [5].

The other possibility is that the inverse electronic compressibility has a point with a Dirac-delta-like negative divergence at some density  $n_c$ . This happens when the free energies of two states which are separated by a barrier, cross each other leading to a cusp singularity. An example is also provided by the EG. Indeed numerical simulations show that the Wigner crystal and the uniform phases free energy cross at some density [16]. Again, the same feature appears in several computations including manganite models [17, 18].

The behavior of  $f_e$  can be summarized by expanding the electronic free energy density  $f_e \equiv F_e/V$  around a reference density  $n_c$  as  $f_e = \alpha|n - n_c|^\gamma$  with  $\alpha < 0$  and corresponds to  $\gamma = 2$  (negative compressibility region) or  $\gamma = 1$  (cusp behavior). A neutral system with  $\alpha < 0$  is unstable toward phase separation, however in a charged system this tendency is frustrated by the long range Coulomb interaction. This leads to the formation of inhomogeneities with a characteristic size  $l_d$  determined by the competition between long range forces and surface energy effects.

Regarding the experiments, the first task is to determine what can be attributed to Coulomb frustrated phase separation and what cannot. Information on the mechanism of the segregation can be obtained by an observation of the

morphology. For example in magnetoresistant manganites, inhomogeneous states with large insulating and/or metallic clusters with very rough interfaces have been reported [19]. These resemble the domains of the random field Ising model where the surface energy plays a role only at very short length scales. The shape of the interfaces is determined by the fluctuations of the local field, which stabilizes one or the other of two competing phases, and long range forces are not needed [20, 21].

A quite different morphology has been observed, also in manganites, by scanning tunneling spectroscopy in thin films. Domains have filamentary and droplike metallic and/or insulating regions on the scale of tens to thousands of nanometers with smooth surfaces indicating strong surface energies [22], which are consistent with Coulomb frustrated phase separation as predicted by Nagaev several years ago [23]. This is reinforced by the fact that the morphology is similar to that of classical mesodomains [1]. Although quenched disorder can have an important role altering the ideal periodic domain configurations that theories predict in the clean limit, the strong dissimilarity with the random field Ising model domain morphology makes it clear that quenched disorder is not the driving force. In this regard it is interesting that, even in the absence of quenched disorder, the complexity of the energy landscape of frustrated phase separation models can make the ordered ground state unreachable, thus leading to a glassy state [24].

It is not clear at the moment which of the two mechanism (quenched disorder or short and long range forces) is dominant in determining each of the anomalous properties of complex electronic systems and more theoretical and experimental work is needed. Several recent experiments, however, point to the important role of short and long range force competition. In the high temperature superconductivity context, scanning tunneling microscopy investigations [25] have revealed an inhomogeneous state of electronic superconducting like nanopatches coexisting with poorly metallic regions. The domains have almost round shapes, indicating that the surface energy has an important role suggesting a Coulomb frustrated phase separation mechanism.

Recently a strong transport anisotropy in ultraclean  $\text{Sr}_3\text{Ru}_2\text{O}_7$  samples has been observed [26]. This striking feature is consistent with the proposal of an exotic electronic liquid phase analogue [27] to the intermediate order states of liquid crystals [28]. The idea that the domains in  $\text{Sr}_3\text{Ru}_2\text{O}_7$  are due to frustrated phase separation has already been put forward [29].

The phenomenology of ruthenates has a strong similarity to that observed in GaAs heterostructures. Several magneto-transport anisotropies arise when the Fermi level lies near the middle of a highly excited Landau level [30]. It has been proposed [31] that in a clean two-dimensional electron gas (2DEG) in high Landau levels, a uniform phase would be unstable against a charge density striped phase where the electron density alternates between zero and full-filling.

Evidence for inhomogeneous states has also been reported in the 2DEG at zero magnetic field. Using a local probe, Ilani and collaborators [32, 33] have shown

that close to the still debated metal–insulator transition (MIT), mesoscopic inhomogeneities appear. In addition thermodynamic measurements have shown that close to the MIT the compressibility departs sharply from the predictions of an homogeneous electron gas [34, 35]. Another interesting finding is the appearance of negative spikes in the electronic compressibility [32] which indicates that the transition from the homogeneous state to the inhomogeneous state is discontinuous, as found theoretically for a striped Coulomb frustrated phase-separated state [36].

In cuprates, as in manganites, the situation is more complex and different inhomogeneities have been reported at different length scales. At a scale of  $\sim 10$  nm,  $\sim 20$  lattice constants, the system appears to segregate into a pseudogap or underdoped phase with a large gap and a superconducting phase with a smaller gap with smooth interfaces in between [25]. This is consistent with Coulomb frustrated phase separation between an underdoped pseudogap phase and an overdoped phase [37]. This scenario has been proposed again in the light of recent neutron scattering experiments [38]. At a scale of  $\sim 4$  lattice constants the systems shows charge ordering in the form of stripes [39]. By considering the  $\text{CuO}_2$  plane as a strongly correlated 2D electronic gas coupled to the lattice, in the presence of the long range Coulomb interaction, it has been proposed [9] that an incommensurate charge density wave occurs around optimal doping as Coulomb frustrated phase separation with hole rich and hole poor regions smoothly evolving into stripes by underdoping.

Since domains in these systems often have mesoscopic scales of several lattice constants, the general aspects of the phenomena can be analyzed by the use of coarse grained models. In this work we will review the two more common coarse grained models corresponding to two different universality classes and their differences and similarities. The paper is organized as follows: In section 2 we review the more relevant models that over the years have been proposed for  $\gamma = 1, 2$  and introduce the basic length scales of the problem. In section 3 we discuss the main properties of phase-separated states for weak Coulomb interaction where a unified picture can be achieved. In section 4 we discuss the strong interaction regime where strong differences between  $\gamma = 1, 2$  arise and we conclude in section 5.

## 2. Minimal models and typical length scales

As discussed in section 1, the tendency for phase separation can be sorted in two main electronic free energy anomalies, corresponding to a negative compressibility density range or a Dirac-delta-like singularity in the compressibility. Although both situations can be captured by expanding the free energy as  $f_e \propto \alpha|n - n_c|^\gamma$  with  $\alpha < 0$  and  $\gamma = 1, 2$ , a full analysis of the phase separation problem, from small to high frustration, requires higher order terms in the free energy expansion as follows:

$$f_e = \alpha|n - n_c|^\gamma + \beta|n - n_c|^{2\gamma}. \quad (1)$$

For  $\beta > 0$  this provides a double-well form for the free energy with minima at  $n = n_c \pm \delta n^0/2$  (here  $\delta n^0 \equiv 2[|\alpha|/(2\beta)]^{1/\gamma}$ )

and a barrier between minima of height  $f_0 = \alpha^2/(4\beta)$ . This form of the free energy assumes two symmetric phases with the same compressibility. One can consider asymmetric situations by adding cubic terms. Such asymmetry does not change the physics substantially and will be neglected for simplicity. The exception is the important case of an incompressible phase coexisting with a compressible phase. This limiting case constitutes a different universality class and will not be discussed here. A treatment can be found in [40] for 3D and in [36] for 2D.

We start by introducing the  $\gamma = 2$  model which is defined by the following free energy:

$$F = \int d^D x [\alpha \Delta n^2 + \beta \Delta n^4 + c |\nabla n(\mathbf{x})|^2] + \frac{Q^2}{2} \int d^D x \int d^D x' [n(\mathbf{x}) - \bar{n}] v(\mathbf{x} - \mathbf{x}') [n(\mathbf{x}') - \bar{n}], \quad (2)$$

where  $\bar{n}$  is the average charge representing the density of the rigid background,  $\Delta n = n - n_c$  and  $v = |\mathbf{x} - \mathbf{x}'|^{-1}$  is the Coulomb interaction. Finally the gradient term models the surface energy of smooth interfaces and is parameterized by the stiffness constant  $c$ . Here the charge density plays the role of a scalar order parameter in an analogous way to the liquid-gas transition of classical fluids. Pattern formation within this model has been considered in [24, 51] in three-dimensional systems, and by Muratov [41], who considered the case of  $D$ -dimensional systems subject to a  $D$ -dimensional Coulomb interaction in the sharp-interface limit. This model is also relevant for describing segregation in block copolymers [4].

Since equation (2) has several parameters, for studying the phase diagram it is convenient to measure lengths in units of  $\xi = \sqrt{2c/\alpha}$ , and define a dimensionless density  $\phi(x) = 2\Delta n(x)/\delta n^0$  and a dimensionless free energy  $\Phi \equiv F/(f_0 \xi^D)$  that, apart from an irrelevant constant, reads:

$$\Phi = \int d^D x [\phi(\mathbf{x})^2 - 1]^2 + |\nabla \phi(\mathbf{x})|^2 + \frac{Q_R^2}{2} \int d^D x \int d^D x' [\phi(\mathbf{x}) - \bar{\phi}] \times v(\mathbf{x} - \mathbf{x}') [\phi(\mathbf{x}') - \bar{\phi}] \quad (3)$$

with  $\bar{\phi} = 2(\bar{n} - n_c)/\delta n^0$  and  $Q_R^2$  a rescaled dimensionless Coulomb coupling given by:

$$Q_R^2 = Q^2 \frac{2\xi^{D-1}}{|\alpha|}.$$

We see that the parameter space can be reduced to only two parameters, the dimensionless global density  $\bar{\phi}$  and the renormalized coupling  $Q_R^2$ . In three-dimensional systems  $Q_R^2$  coincides with the dimensionless coupling introduced in [41, 51].

The  $\gamma = 1$  case has been investigated with approximate treatments in three- [42, 40] and two-dimensional systems [36] and within an exactly solvable model in the limit  $\beta = 0$  [43] and  $\beta \neq 0$  [44]. In this case frustrated phase separation is more easily described by adding an auxiliary field  $s$  linearly coupled to the charge and analogous to a

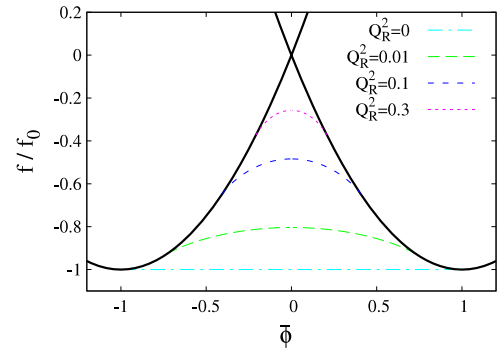


**Figure 1.** Behavior of the free energy densities of the electronic uniform phases for the  $\gamma = 1$  model equation (5) and  $D = 2$ . The dashed lines are the exact energy of stripe inhomogeneities for different values of the frustrating parameter. The short-long dashed line corresponds to the Maxwell construction ( $Q_R^2 = 0$ ).

Hubbard–Stratonovich variable. Two versions of the model are possible which lead to similar results:  $s$  can be taken as a soft or a conventional Ising spin with  $s = \pm 1$  where the sign distinguishes the two competing phases. We take the latter model which is more straightforward to analyze. It consists of a ferromagnetic Ising model linearly coupled to the local charge:

$$F = -J \sum_{\langle ij \rangle} (s_i s_j - 1) - |\alpha| \sum_i s_i (N_i - N_c) + \frac{\beta}{a^D} \sum_i (N_i - N_c)^2 + \frac{Q^2}{2} \sum_{ij} (N_i - \bar{N}) v(\mathbf{x}_i - \mathbf{x}_j) (N_j - \bar{N}) \quad (4)$$

where  $s_i = \pm 1$ , the index  $i$  runs over the sites of a hypercubic lattice of dimension  $D = 2, 3$  with lattice constant  $a$ , the  $N_i$  are dimensionless numbers of particles per site and  $\bar{N}$  their average value. The soft version replaces the Ising part with a double-well potential [43].

We have written the model in the lattice for clarity but we are interested on the continuum limit of this model with  $n(\mathbf{x}) \equiv N_i/a^D$ . Uniform phases correspond to a ferromagnetic state in  $s$ . Inserting the two possible values of  $s$  in equation (4) one obtains that uniform phases are described by equation (1) with  $\gamma = 1$ , i.e. two intersecting parabolas with minima at  $\pm \delta n_0/2$  and a crossing point at  $n_c$  (the full lines in figure 1). In the hard spin case domain walls of the Ising order parameter are sharp by construction with a surface tension  $\sigma = 2J/a^{D-1}$ , thus the Ising term can be written as  $\sigma \Sigma$  with  $\Sigma$  the total surface of interface among the two phases. It is convenient to define the analogue of  $\xi$  for the present model  $\xi \equiv 4\sigma\beta/\alpha^2$ . This represents the size that inhomogeneities should have for the total interface energy be of the same order as the phase separation energy density gain  $\alpha^2/(4\beta)$ . As before we measure the energy in units of  $\xi^D \alpha^2/(4\beta)$ , lengths in units of  $\xi$  and surfaces in units of  $\xi^{D-1}$ . In these units  $\sigma \equiv 1$  and apart from an irrelevant constant one obtains the following free

energy functional:

$$\begin{aligned} \Phi = & \Sigma + \int d^D x [\phi(\mathbf{x}) - s(\mathbf{x})]^2 \\ & + \frac{Q_R^2}{2} \int d^D x \int d^D x' [\phi(\mathbf{x}) - \bar{\phi}] \\ & \times v(\mathbf{x} - \mathbf{x}') [\phi(\mathbf{x}') - \bar{\phi}], \end{aligned} \quad (5)$$

where

$$Q_R^2 = Q^2 \frac{\xi^{D-1}}{\beta}.$$

As for the model equation (3) the parameter space is determined by the two dimensionless parameters  $\bar{\phi}$  and  $Q_R^2$ . Frustration can be also measured by the parameter  $Q_R^{2/D}$  which, as shown below, has the meaning of the ratio between the energy cost introduced by frustration and phase separation energy gain. This was the parameter used in [42, 40, 36, 44].

In the absence of the Coulomb interaction, both models are subject to ordinary phase separation in a range of global densities  $|\bar{\phi}| < 1$  as determined by the Maxwell (or ‘tangent’) construction shown by the short–long dashed line in figure 1. The phase-separated state is made up of macroscopic domains with constant local densities  $\phi = \pm 1$ . For  $Q_R^2 \neq 0$ , macroscopic phase separation is precluded since the Coulomb cost grows faster than the volume in the thermodynamic limit and mesoscale domains appear.

The typical size of the domains  $l_d$  can be obtained by dimensional analysis. We define  $\tilde{l}_d \equiv l_d/\xi$ . Taking  $\phi \sim 1$  the Coulomb cost per domain can be estimated making the integrals in a volume of order  $\tilde{l}_d^D$  as  $Q_R^2 \tilde{l}_d^{2D-1}$ . The surface energy goes as  $\tilde{l}_d^{D-1}$ . Both quantities are optimized when the inhomogeneities have the size defined by

$$\tilde{l}_d^D = 1/Q_R^2. \quad (6)$$

Another important length scale is the screening length of the Coulomb interaction that can be defined for two- and three-dimensional systems as:

$$l_s^{D-1} = [2^{D-1} \pi Q^2 \kappa]^{-1}, \quad (7)$$

where  $\kappa$  is a characteristic electronic compressibility of the competing homogeneous phases:

$$\kappa = (2\beta)^{-1} \quad (\gamma = 1) \quad (8)$$

$$\kappa = (2|\alpha|)^{-1} \quad (\gamma = 2). \quad (9)$$

For both the models presented above the characteristic screening length in units of  $\xi$  can be defined as

$$\tilde{l}_s^{D-1} \equiv 1/Q_R^2. \quad (10)$$

At weak frustration  $Q_R \ll 1$  we have the following hierarchy of scales [41] (cf equations (6), (10)):

$$l_s \gg l_d \gg \xi. \quad (11)$$

This separation of lengths allows for a unified treatment of the frustrated phase separation mechanism at weak frustration that will be discussed in the following section.

### 3. The weak frustration regime

In the weak frustration regime, the effect of long range forces can be considered as a small perturbation upon the ordinary phase separation mechanism. Thus, mixed states are expected to appear, with local densities close to the two minima of the double well. For systems with  $\gamma = 2$ , frustrated phase separation can be analyzed by expanding quadratically the free energy around the two densities  $\phi = \pm 1$ . Then the bulk free energy becomes the same as for the  $\gamma = 1$  model. In addition, the hierarchy of length scales equation (11) for  $Q_R^2 \ll 1$  allows one to consider the interface as sharp. A surface tension can be defined by computing the excess energy of an isolated interface [41]. At this point, the two models become equivalent. In the remainder we present the analysis of the  $\gamma = 1$  model which can be solved analytically for stripes in  $D = 2$  and layers in  $D = 3$ .

Before discussing the exact solution, it is convenient to discuss an approximate solution which gives essentially the same result as the exact solution in weak coupling but in addition allows the consideration of other geometries. Since the state is expected to be similar to the macroscopically phase-separated state one can take a uniform density approximation (UDA) in which the local density inside the domains is assumed constant [42, 12, 40, 36, 44]. Comparison with the exact result shows that this gives very accurate results in two- and three-dimensional systems [44].

The low (high) density phase will be termed  $A$  ( $B$ ). Defining  $\tilde{f} \equiv f/f_0$  the free energy density can be written as:

$$\tilde{f} = (1 - \nu) \tilde{f}_A(\phi_A) + \nu \tilde{f}_B(\phi_B) + e_{\text{mix}}, \quad (12)$$

where  $\tilde{f}_{A/B} = (\phi \pm 1)^2$  and  $\nu$  indicates the volume fraction of the  $B$ -phase domains.  $e_{\text{mix}}$  represents the additional energetic cost to form inhomogeneities due to the long range Coulomb interaction and the interface boundary energy. For a given geometry it is determined by adding the Coulomb cost and the surface energy cost and optimizing with respect to the dimension of the inhomogeneities. It can be cast as:

$$e_{\text{mix}} = Q_R^{2/D} (\phi_B - \phi_A)^{2/D} u(\nu). \quad (13)$$

The dependence of the mixed states (MS) free energy upon the morphology of the domains is stored in the function  $u(\nu)$ . In figure 2 we plot  $u(\nu)$  for the different geometries. These functions have been evaluated in [42, 36] and appear also in the theory of diblock copolymers [4]. The advantage of the UDA approximation is that the mixing energy, which includes the long range force effects, can be computed independently from the specific modeling of the homogeneous phases free energy. These functions are valid whatever form one chooses for  $f_{A/B}$ .

As shown in figure 2 droplet-like or disk inhomogeneities are preferred for low volume fractions of the minority phase ( $\nu \sim 0$  or  $\nu \sim 1$ ). On the contrary stripes and layers appear for  $\nu \sim \frac{1}{2}$ . At intermediate values of  $\nu$  in three-dimensional systems one finds cylindrical rods. In the diblock copolymer context the control parameter is the volume fraction  $\nu$ . Here instead the control parameter is the global density  $\bar{\phi}$ . However for  $Q_R^2 \ll 1$ , the volume fraction increases nearly linearly

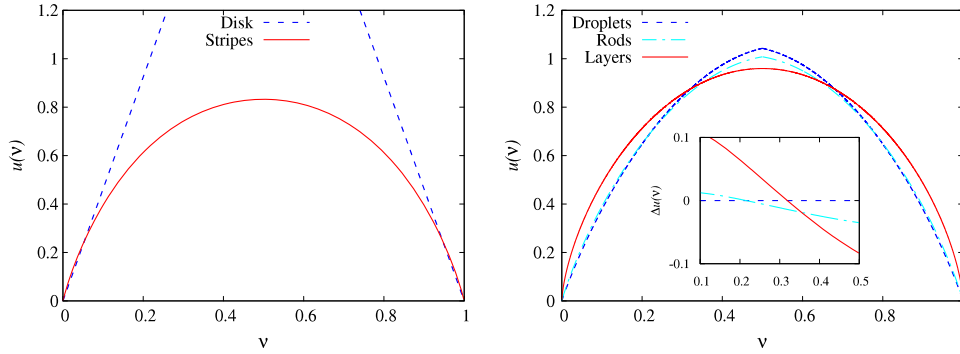


**Figure 2.** The left (right) panel shows the function  $u(v)$  in two- (three-)dimensional systems for stripes and disks (layers, rods and droplets). For the disk, droplet and rod inhomogeneities, the mixing energy has been computed referring to  $B$ -phase inhomogeneities for  $v < \frac{1}{2}$  while  $A$ -phase droplets and rods has been considered for  $v > \frac{1}{2}$ . The inset in the right panel shows the difference in  $u$  with respect to the droplet geometry to resolve the crossings between the different morphologies.

with the global density and the two parameters are practically equivalent. From figure 2 one sees that there will be a series of morphological transitions that connect droplet states near the homogeneous–MS transitions to the striped mixed state at  $\bar{\phi} \sim 0$ . In the present approximation they appear as first order, however consideration of more complicated geometries and charge relaxation effects can change this to a smooth evolution of inhomogeneities that could also include ‘fingering’ and elongation of the domains as in classical systems [1]. The stripe and rod phases are expected to behave as a glass in quench experiments [24] with labyrinth-like patterns.

Since we are measuring energies in terms of the barrier height, which represents the characteristic energy gain from the phase separation equation (13) allows one to give another physical interpretation to the frustration parameter:

$$Q_R^2 = \left( \frac{\text{Char. mixing energy cost}}{\text{Char. phase separation energy gain}} \right)^D.$$

In figure 1 we show with dashed lines the typical behavior of mixed states (MS) free energies for the  $\gamma = 1$  model at different values of  $Q_R^2$ . These results are exact but the results within the UDA approximation at weak frustration are practically identical [44]. An interesting property of mixed states is that they present the ‘wrong’ curvature; that is, the electronic compressibility  $\partial^2 f_e / \partial \phi^2$  is negative. Generally, this does not imply a thermodynamic instability since the usual stability condition of positive compressibility must be formulated for the global neutral system, thus including the background compressibility. Since in frustrated phase separation analysis, the inverse background compressibility is assumed to be an infinite positive number (the background density is fixed to the uniform average value  $\bar{\phi}$ ), it follows from this point of view that the system is in a stable MS.

An important difference with ordinary phase separation resides in the behavior of the local densities of the domains. In unfrustrated phase separation the two phases have a constant density independently of the global density. In frustrated phase separation the local density of the domains decreases with an increase of the global density [42, 40]. Assuming that the Curie temperature is an increasing function of the local density,

rather than the global density (controlled by doping), this could explain [12] the puzzling maximum of the Curie temperature in the three-dimensional perovskite manganite  $\text{La}_{1-x}\text{Ca}_x\text{MnO}_3$  at  $x = 0.35$  Ca doping [45] which is not predicted by the conventional double-exchange mechanism [46–48].

#### 4. The strong frustration regime

The results presented above, fully determine the behavior of MS in the weak frustration regime. By increasing the renormalized Coulomb frustration in the model equations (3), (5), MS with local densities close to the reference density appear. In this case the behavior of the two models is radically different leading to two ‘universality’ classes.

We start by analyzing the  $\gamma = 1$  universality class. As a first approximation we can invoke the UDA, keeping in mind that in this case, since we are far from the Maxwell construction limit, the results should be taken with a pinch of salt. Indeed we will see that special care is needed for  $D = 2$ .

For simplicity we fix the global density at the reference density  $\bar{\phi} = 0$  and look for the energetic stability of a striped ( $D = 2$ ) or layered ( $D = 3$ ) mixed state. By symmetry  $v = 1/2$  and the free energy density behaves as

$$\delta \tilde{f} = -|\delta\phi| + \frac{1}{4}\delta\phi^2 + Q_R^{2/D} u(1/2)\delta\phi^{2/D} \quad (\gamma = 1), \quad (14)$$

where  $\delta\phi = \phi_B - \phi_A$ . The first term represents the phase separation energy gain, the second term is an energetic cost due to compressibility effects and the last term is the UDA mixing energy (cf equation (13)). The condition of stability of mixed states reads  $\delta \tilde{f} < 0$ . For  $D = 3$  the last term is dominant at small  $\delta\phi$  and combined with the linear term produces an energetic barrier between the homogeneous state ( $\delta\phi = 0$ ) and the inhomogeneous state ( $\delta\phi \neq 0$ ). The quadratic term ensures stability for large  $\delta\phi$ . Clearly the transition will be first order with a critical frustration given by  $Q_{R,c}^2 = 27/[4u(1/2)]^3 \sim 0.47$ . Apart from small numerical corrections this result coincides with the exact solution (cf figure 3). The different power dependence of the phase separation energy gain and the mixing energy cost makes the UDA reliable.

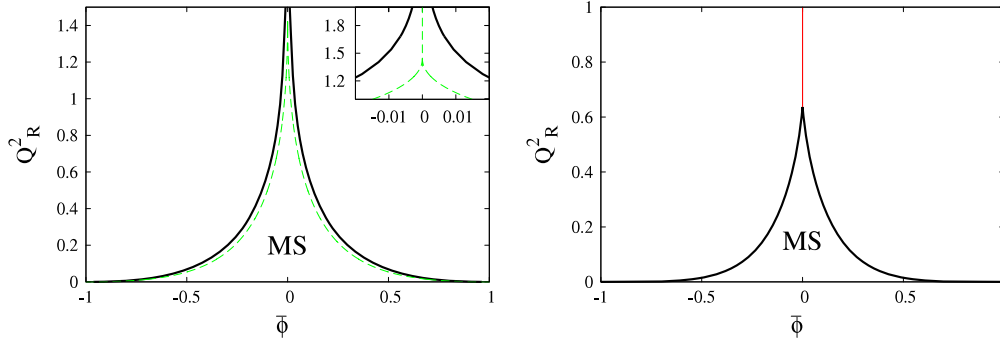


**Figure 3.** The full line in the left (right) panel represents the exact phase diagram of the  $\gamma = 1$  model for a smectic striped (layered) state in a two- (three-) dimensional system. The dashed line in the left panel represents the UDA approximation. A discrepancy between the two solutions is found for  $Q_R^2 \sim Q_{R,c}^2$  (inset of the left panel) since the UDA predicts a critical value of  $Q_R^2$  while the exact model shows a logarithmic singularity. In three-dimensional systems the UDA (not shown) gives qualitatively the same result as the exact solution. For  $Q_R^2 > Q_{R,c}^2$  there is a common boundary (thin line) between the two homogeneous phases.

Another important prediction of the UDA is that domains never have all linear dimensions much larger than the screening length. This important result is quite general and can be derived by simple arguments (see below). A small difference between the UDA and the exact results arises exponentially close to  $(Q_{R,c}^2, \bar{\phi}_c = 0)$  where domains with  $l_d \gg l_s$  are possible. This region however is physically irrelevant since it requires an unphysical tuning of the density.

For  $D = 2$  we are in a marginal situation. There is a delicate balance between the first and the third terms in equation (14) which are of the same order. The transition looks second order with  $Q_{R,c}^2 = 1/u(1/2)^2 \sim 1.45$ . This result, however, is incorrect. In this marginal case charge relaxation introduces a correction which unbalances the two terms. Fortunately the model is analytically solvable [43, 44] for the stripe and layered structures which are the expected morphologies close to  $\bar{\phi} = 0$ . In figure 3 we show the exact phase diagrams for these particular morphologies in two- and three-dimensional systems. For  $D = 2$  the transition lines diverge logarithmically at  $\bar{\phi} = 0$  and there is no upper limit for the mixed state. Therefore a direct first-order phase transition between homogeneous phases is not possible and there is always an intermediate phase.

The same result was first obtained in this region of the phase diagram by neglecting the compressibility term in the free energy  $\propto \phi^2$  [43]. Indeed, in the strong frustrating regime the typical size of 2D domains is exponentially larger than the screening length and thus the physics is determined by the slow power-law relaxation of the charge density (figure 4). The screening length plays the role of a short length cutoff that removes the unphysical divergence of the charge density at the domain boundaries arising at  $\beta = 0$ .

From a practical point of view, the strongly frustrated 2D mixed state can be quite difficult to observe. It appears in the exponentially narrow range of densities

$$|\bar{\phi}| < e^{-Q_R^2/4}$$

and therefore it requires an extremely accurate control of the density. It may be possible that this is achieved to some extent

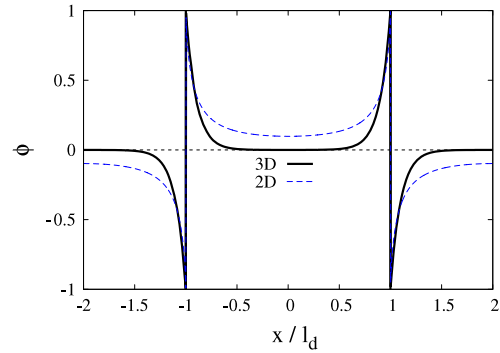


**Figure 4.** Behavior of the charge density modulation at the reference density  $\bar{\phi} = 0$  for a cut perpendicular to the stripes in two-dimensional systems and the layers in three-dimensional systems and domain width  $W = 20l_s$ .

in ruthenates, where the control parameter is the magnetic field, which allows for considerable fine tuning, and the system is ultraclean.

Another difficulty is that the inverse electronic compressibility

$$\kappa_{MS}^{-1} \propto \frac{-\kappa^{-1} e^{Q_R^2/4}}{\sqrt{1 - (e^{Q_R^2/4} \bar{\phi})^2}}$$

is exponentially large and negative in all the mixed state stability range and negatively diverges with  $1/2$  critical exponent at the transition. As stated in section 3, in frustrated phase separation models the background is assumed incompressible ( $\kappa_b \equiv 0$ ), however real systems will have a small finite background compressibility  $\kappa_b > 0$ . This will lead to a volume instability analogous to the volume instability of cerium metal [42, 49].

In some cases, when there is a large separation of energy scales, the background may behave as nearly incompressible. This can occur in ruthenates where the relevant electronic phenomena occur at temperatures below a tenth of a kelvin as compared with the melting temperature of the material of the order of hundreds of kelvin. In the case of a 2D electron gas with an ionic background there is also a similar separation

of energy scales. In addition, from an elastic point of view, the background is three dimensional and therefore behaves as practically incompressible. In field-effect-transistors where the background is made of mobile charges, the situation is quite different and the background compressibility cannot be neglected [50].

Differences arising between two- and three-dimensional systems are mainly due to the different behavior of the charge density profile inside the domains. The phase separation energy gain stems from the region where the electronic density is significantly different from its average value [42]. In two-dimensional systems the power-law behavior of the charge density allows a gain of phase separation energy even far from the boundaries. On the contrary, in three-dimensional systems the charge density decays exponentially from the domain boundary on the scale of the Thomas–Fermi screening length (figure 4). Thus the system gains phase separation energy in a range of the order of the screening length from the domain boundaries. Regions far from the boundaries produce an exponentially small energy gain. Thus if phase separation is favorable the system adjusts itself in such a way to eliminate all these regions. Domains satisfy a maximum size rule such that every point of the domain is at a distance of the order of the screening length or smaller from the boundaries. This rule proves to be quite general and is independent of the model. The maximum size rule allows arbitrary large inhomogeneities in two-dimensional systems since one of the dimensions is already smaller than  $l_s^{3D}$ .

Now we discuss the case of  $\gamma = 2$  at strong frustration. The separation of length scales discussed in section 3 is no longer valid, the UDA becomes unreliable and the effect of smooth interfaces plays a prominent role.

Computing the static response to an external field in momentum space one obtains the following charge susceptibility:

$$\chi(q) = \left[ q^2 - 2 + 6\bar{\phi}^2 + \frac{Q_R^2}{2} v(q) \right]^{-1}.$$

We recall that the system is considered to be  $D$ -dimensional but embedded in the usual three-dimensional Coulomb interaction. The Fourier transform reads:

$$v(q) = \frac{2^{D-1}\pi}{|q|^{D-1}}.$$

$\chi$  diverges for  $D = 2, 3$  at a characteristic finite wavevector  $q_c$  on a Gaussian instability line  $Q_R^2(\bar{\phi})$ . Above  $Q_{R,c}^2 = 1/(2\pi)$  in 3D and  $Q_{R,c}^2 = (4\sqrt{2})/(3\sqrt{3}\pi)$  in 2D, the system is always homogeneous. On entering the unstable region at  $|\bar{\phi} = 0$ , a sinusoidal charge density wave (SCDW) occurs. Away but close to  $|\bar{\phi} = 0$  the transition is weakly first order with more complicated morphologies but smooth interfaces. Thus inhomogeneities are quite different from the mesodomains of the weak coupling regime (section 3). The crossover between these two regimes is discussed in [51]. In anisotropic systems both in 3D and in 2D, when the modulation can occur in one direction only, SCDW extends away from  $\bar{\phi} = 0$  and switches to a first order transition via a tricritical point.

A related mechanism has been proposed in cuprates to predict the charge ordering instabilities and other anomalous properties in accord with experiment [9]. In classical systems this is often referred to as the ‘microphase’ separation transition [1, 41].

## 5. Conclusions

In this work we reviewed the main aspects of frustrated phase separation in charged systems by considering two kind of compressibility anomalies that generally occur in strongly correlated systems. For the different coarse grained models that have been introduced in the literature, the outcome of long range forces can be measured by a dimensionless parameter that defines the amount of frustrating effects. Frustration tends to reduce the range of density where a mixed state appears. Thus uniform phases are possible at densities where, in the absence of long range forces, phase separation would occur. This situation is in accord with thermodynamic measurements [34, 35] of the uniform 2DEG, where one finds stability of the uniform phase with negative compressibility.

In the presence of frustration the mixed state consists of domains of mesoscopic size with various geometries depending on the control parameters. A sequence of morphological transitions occurs that has a strong similarity to those in other systems [1, 4].

When frustrating effects are small perturbations, a unified description of MS is allowed and a simple approximation, in which the density inside the domains is assumed constant, gives very accurate results.

At strong frustration, the properties of the mixed state strongly depends upon the particular anomaly in the compressibility and one can define two different universality classes. For systems with a cusp singularity in the electronic compressibility ( $\gamma = 1$ ) the system dimensionality plays a key role in the charge segregation mechanism. A critical frustration  $Q_{R,c}$ , above which mixed states are not possible, exists only for  $D = 3$ .

In systems with a negative electronic compressibility region ( $\gamma = 2$ ) a critical value of the frustration exists  $Q_{R,c}$  for both  $D = 2, 3$ . In anisotropic systems, close to  $Q_{R,c}$  the inhomogeneities are SCDW.

The maximum size rule says that domains cannot have all linear dimensions much larger than the screening length independently of  $Q_R$ . Thus a necessary condition for the applicability of a coarse grained treatment is that the three-dimensional screening length must be much greater than the typical microscopic lengths, such as the interparticle distance and the lattice constant. Therefore mesoscopic domains can be expected in systems with small compressibility, such as bad metals or systems close to metal–insulator transitions, or systems with very anisotropic electronic properties (i.e. are nearly insulating in one direction). Interestingly most of the materials where mesoscopic domains have been found have these characteristics.

*Note added in proof.* After this work was finished the phase diagram of the  $\gamma = 2$  model has been completely characterized in [51].

## References

- [1] Seul M and Andelman D 1995 *Science* **267** 476
- [2] Kittel C 1946 *Phys. Rev.* **70** 965
- [3] Landau L D and Lifshitz E M 1984 *Electrodynamics of Continuous Media* (New York: Pergamon)
- [4] Ohta T and Kawasaki K 1986 *Macromolecules* **19** 2621
- [5] Lorenz C P, Ravenhall D G and Pethick C J 1993 *Phys. Rev. Lett.* **70** 379
- [6] Mahan G D 2000 *Many Particle Physics* 3rd edn (New York: Plenum)
- [7] Nagaev E L 1967 *JETP Lett.* **6** 18
- [8] Markiewicz R S 1990 *J. Phys.: Condens. Matter* **2** 665
- [9] Castellani C, Di Castro C and Grilli M 1995 *Phys. Rev. Lett.* **75** 4650
- [10] van Dongen P G J 1995 *Phys. Rev. Lett.* **74** 182
- [11] Kagan M Y, Khomskii D I and Mostovoy M V 1999 *Eur. Phys. J. B* **12** 217
- [12] Lorenzana J, Castellani C and Di Castro C 2001 *Phys. Rev. B* **64** 235128
- [13] Freericks J K, Lieb E H and Ueltschi D 2002 *Phys. Rev. Lett.* **88** 106401
- [14] Kugel K I, Rakhmanov A L and Sboychakov A O 2005 *Phys. Rev. Lett.* **95** 267210
- [15] Fishman R S, Reboredo F A, Brandt A and Moreno J 2007 *Phys. Rev. Lett.* **98** 267203
- [16] Ceperley D M and Alder B J 1980 *Phys. Rev. Lett.* **45** 566
- [17] van den Brink J, Khaliullin G and Khomskii D 1999 *Phys. Rev. Lett.* **83** 5118
- [18] Okamoto S, Ishihara S and Maekawa S 2000 *Phys. Rev. B* **61** 451
- [19] Fäth M, Freisem S, Menovsky A A, Tomioka Y, Aarts J and Mydosh J A 1999 *Science* **285** 1540
- [20] Dagotto E, Hotta T and Moreo A 2001 *Phys. Rep.* **344** 1
- [21] Burgy J, Mayr M, Martin-Mayor V, Moreo A and Dagotto E 2001 *Phys. Rev. Lett.* **87** 277202
- [22] Becker T, Streng C, Luo Y, Moshnyaga V, Damaschke B, Shannon N and Samwer K 2002 *Phys. Rev. Lett.* **89** 237203
- [23] Nagaev E L 1983 *Physics of Magnetic Semiconductors* (Moscow: Mir)
- [24] Schmalian J and Wolynes P G 2000 *Phys. Rev. Lett.* **85** 836
- [25] Lang K M, Madhavan V, Hoffman J E, Hudson E W, Eisaki H, Uchida S and Davis J C 2002 *Nature* **415** 412
- [26] Borzi R A, Grigera S A, Farrell J, Perry R S, Lister S J S, Lee S L, Tennant D A, Maeno Y and Mackenzie A P 2007 *Science* **315** 214
- [27] Kivelson S A, Fradkin E and Emery V J 1998 *Nature* **393** 550
- [28] Chaikin P M and Lubensky T C 1995 *Principles of Condensed Matter Physics* (Cambridge: Cambridge University Press)
- [29] Honerkamp C 2005 *Phys. Rev. B* **72** 115103
- [30] Lilly M P, Cooper K B, Eisenstein J P, Pfeiffer L N and West K W 1999 *Phys. Rev. Lett.* **83** 824
- [31] Koulakov A A, Fogler M M and Shklovskii B I 1996 *Phys. Rev. Lett.* **76** 499
- [32] Ilani S, Yacoby A, Mahalu D and Shtrikman H 2001 *Science* **292** 1354
- [33] Ilani S, Yacoby A, Mahalu D and Shtrikman H 2000 *Phys. Rev. Lett.* **84** 3133
- [34] Eisenstein J P, Pfeiffer L N and West K W 1992 *Phys. Rev. Lett.* **68** 674
- [35] Eisenstein J P, Pfeiffer L N and West K W 1994 *Phys. Rev. B* **50** 1760
- [36] Ortix C, Lorenzana J and Di Castro C 2006 *Phys. Rev. B* **73** 245117
- [37] Lorenzana J and Seibold G 2002 *Phys. Rev. Lett.* **89** 136401
- [38] Wakimoto S, Yamada K, Tranquada J M, Frost C D, Birgeneau R J and Zhang H 2007 *Phys. Rev. Lett.* **98** 247003
- [39] Tranquada J M, Sternlieb B J, Axe J D, Nakamura Y and Uchida S 1995 *Nature* **375** 561
- [40] Lorenzana J, Castellani C and Di Castro C 2002 *Europhys. Lett.* **57** 704
- [41] Muratov C B 2002 *Phys. Rev. E* **66** 066108
- [42] Lorenzana J, Castellani C and Di Castro C 2001 *Phys. Rev. B* **64** 235127
- [43] Jamei R, Kivelson S and Spivak B 2005 *Phys. Rev. Lett.* **94** 056805
- [44] Ortix C, Lorenzana J, Beccaria M and Di Castro C 2007 *Phys. Rev. B* **75** 195107
- [45] Schiffer P, Ramirez A P, Bao W and Cheong S-W 1995 *Phys. Rev. Lett.* **75** 3336
- [46] Zener C 1951 *Phys. Rev.* **82** 403
- [47] Anderson P W and Hasegawa H 1955 *Phys. Rev.* **100** 675
- [48] de Gennes P G 1960 *Phys. Rev.* **118** 141
- [49] Bustingorry S, Jagla E and Lorenzana J 2003 *Preprint cond-mat/0307134*
- [50] Spivak B 2003 *Phys. Rev. B* **67** 125205
- [51] Ortix C, Lorenzana J and Di Castro C 2008 *Phys. Rev. Lett.* **100** 246402